HUHS1015 Suppresses Colonic Cancer Growth by Inducing Necrosis and Apoptosis in Association with Mitochondrial Damage

YOSHIKO KAKU[1*], AYAKO TSUCHIYA[1*], TADASHI SHIMIZU[2], AKITO TANAKA[2] and TOMOYUKI NISHIZAKI[1]

[1]*Division of Bioinformation, Department of Physiology and Division of Respiratory Medicine, Hyogo College of Medicine, Mukogawa-cho, Nishinomiya, Japan;*
[2]*Laboratory of Chemical Biology, Advanced Medicinal Research Center, Hyogo University of Health Sciences, Minatojima, Chuo-ku, Kobe, Japan*

Abstract. *Background: The newly-synthesized naftopidil analog HUHS1015 suppresses tumor growth and induces apoptosis of cells from a variety of cancer types. The present study was conduced to assess the effect of HUHS1015 on human colonic cancer cells and to clarify the underlying mechanism. Results: HUHS1015 reduced cell viability of Caco-2 and CW2 human colonic cancer cell lines in a concentration (0.3-100 mM)-dependent manner. HUHS1015 increased terminal deoxynucleotidyl transferase-mediated dUTP nick-end labeling-positive cells in both cell lines. In flow cytometry using propidium iodide and annexin V, HUHS1015 significantly increased the populations of cells undergoing primary necrosis, early apoptosis, and late apoptosis/secondary necrosis in both cell lines. In the cell-cycle analysis, HUHS1015 increased the proportion of the sub-G_1 phase of cell, which corresponds to apoptotic cells. HUHS1015 perturbed the mitochondrial membrane potential and reduced the intracellular ATP level. HUHS1015 activated caspases 3, -4, -8, and -9, particularly caspase-3. HUHS1015 promoted cytochrome c release from the mitochondria. HUHS1015 significantly inhibited tumor growth in mice inoculated with CW2 cells. Conclusion: HUHS1015 induces necrosis by lowering the intracellular ATP level in association with mitochondrial damage and caspase-dependent apoptosis. This occurs in part by stimulating cytochrome c release from the mitochondria to activate caspase-9 followed by the effector caspase-3, responsible for suppression of colonic cancer proliferation in the mouse xenograft model.*

Naftopidil, an antagonist for a1-adrenoceptor, is clinically used for treatment of benign prostate hyperplasia and hypertension (1). Recently it has been discussed whether naftopidil may serve as an anticancer drug. Naftopidil reduced cell viability of bladder, prostate, and renal cancer cell lines, and induced apoptosis in malignant pleural mesothelioma cell lines (2, 3). Amazingly, the protein kinase C inhibitor GF109203X attenuates naftopidil-induced apoptosis of malignant mesothelioma cells, and cell proliferation was stimulated by knocking-down a1D-adrenoceptor (3). This suggests that naftopidil induces apoptosis of malignant mesothelioma cells by a mechanism independent of a1-adrenoceptor blocking.

To develop a new anticancer drug, we synthesized 21 naftopidil analogs. Out of them, we obtained 1-[2-(2-methoxy-phenylamino)ethylamino]-3-(naphthalene- 1-yloxy)propan-2-ol (HUHS1015), which exhibited the most beneficial antitumor effect among the synthesized naftopidil analogs. HUHS1015 induces cell death in a variety of cancer cell types, which include human malignant mesothelioma cell lines NCI-H28, NCI-H2052, NCI-H2452, and MSTO-211H; human lung cancer cell lines A549, SBC-3, and Lu-65; human hepatoma cell lines HepG2 and HuH-7; human gastric cancer cell lines MKN28 and MKN45; human bladder cancer cell lines 253J, 5637, KK-47, TCCSUP, T24, and UM-UC-3s; human prostate cancer cell lines DU145, LNCaP, and PC-3; and human renal cancer cell lines ACHN, RCC4-VHL, and 786-O (4, 5). Intriguingly, HUHS1015 induced caspase-independent and -dependent apoptosis of MKN28 and MKN45 cells, respectively, and effectively suppressed MKN45 cell proliferation (6). Moreover, HUHS1015 induced necroptosis

*These Authors contributed equally to this study.

Correspondence to: Professor Tomoyuki Nishizaki, MD, Ph.D., Division of Bioinformation, Department of Physiology, Hyogo College of Medicine, 1-1 Mukogawa-cho, Nishinomiya 663-8501, Japan. Tel: +81 798456397, Fax: +81 798456649, e-mail: tomoyuki@hyo-med.ac.jp

Key Words: HUHS1015, necrosis, apoptosis, colonic cancer cell.

and caspase-independent apoptosis of MKN28 cells in association with accumulation of apoptosis-inducing factor-homologous mitochondrion-associated inducer of death (AMID) in the nucleus (7).

The present study investigated the anticancer effect of HUHS1015 on Caco-2 and CW2 human colonic cancer cell lines and the underlying mechanism. We showed that HUHS1015 induces both mitochondria-mediated necrosis and apoptosis of colonic cancer cells by lowering intracellular ATP levels and stimulating cytochrome *c* release to activate caspase-9 followed by the effector caspase-3. It was also shown that HUHS1015 has a beneficial anticancer effect on CW2 cell proliferation in the mouse xenograft model.

Materials and Methods

Animal care. All procedures were approved by the Animal Care and Use Committee at Hyogo College of Medicine (12-071) and were in compliance with the National Institutes of Health Guide for the Care and Use of Laboratory Animals.

Cell culture. Caco-2 and CW2 cell lines were obtained from RIKEN cell bank (Ibaraki, Japan). Cells were cultured in a Dulbecco's modified Eagle's medium supplemented with 10% heat-inactivated fetal bovine serum, penicillin (final concentration, 100 U/ml), and streptomycin (final concentration, 0.1 mg/ml), in a humidified atmosphere of 5% CO_2 and 95% air at 37˚C.

Cell viability. Cell viability was evaluated by the 3-(4,5-dimethyl-2-thiazolyl)- 2,5-diphenyl-2*H*-tetrazolium bromide (MTT) method, as previously described (8). Cells were incubated in the solution without (controls) and with HUHS1015 in the presence and absence of necrostatin-1 (Nec-1).

Terminal deoxynucleotidyl transferase-mediated dUTP nick-end labeling (TUNEL) staining. TUNEL staining was performed to detect *in situ* DNA fragmentation as a marker of apoptosis using an In Situ Apoptosis Detection Kit (Takara Bio, Shiga, Japan). Briefly, fixed and permeabilized cells were reacted with terminal deoxynucleotidyl transferase and fluorescein isothiocyanate (FITC)-deoxyuridine triphosphate for 90 min at 37˚C. FITC signals were visualized with a confocal scanning laser microscope (LSM 510; Carl Zeiss Co., Ltd., Oberkochen, Germany).

Apoptosis assay. Cells were suspended in a binding buffer and stained with both propidium iodide (PI) and annexin V (AV)-FITC, and loaded onto a flow cytometer (FACSCalibur; Becton Dickinson, Franklin Lakes, NJ, USA) available for FL1 (AV) and FL2 (PI) bivariate analyisis. Data from 20,000 cells/sample were collected, and the quadrants were set according to the population of viable, unstained cells in untreated samples. CellQuest (Becton Dickinson) analysis of the data was used to calculate the percentage of the cells in the respective quadrants.

Cell-cycle analysis. Cells were harvested by a trypsinization, then fixed with 70% (v/v) ethanol at 4˚C overnight. Fixed cells were incubated in phosphate-buffered saline (PBS) containing 1.5 mg/ml RNase A for 1 h at 37˚C, followed by staining with 50 mg/ml of PI for 20 min on ice. Then cells were collected on a nylon mesh filter (pore size, 40 mm), and cell cycles were assayed with a flow cytometer (FACSCalibur) at an excitation of 488 nm and an emission of 585 nm, and analyzed using a BD CellQuest Pro software (Becton Dickinson).

Monitoring of mitochondrial membrane potential. Cells were incubated in a DePsipher™ (Trevigen, Inc., Gaithersburg, MD, USA) solution at 37˚C for 20 min, and washed with a reaction buffer with a stabilizer solution. The fluorescent signals were observed with a confocal scanning laser microscope (LSM 510; Carl Zeiss Co., Ltd.) through a long-pass 560 nm filter for red aggregations and 488 nm argon laser and band-pass 505-530 nm filter for green monomeric form at 543 nm Helium-Neon laser. Red fluorescence is emitted from the red aggregates of DePsipher, which are formed within mitochondria in healthy cells. Green fluorescence reveals the monomeric form of the DePsipher molecule, which appears in the cytosol after mitochondrial membrane depolarization.

Real-time reverse transcription-polymerase chain reaction (RT-PCR). Total RNAs from cells were purified by an acid/guanidine/thiocyanate/chloroform extraction method using the Sepasol-RNA I Super kit (Nacalai, Kyoto, Japan). After purification, total RNAs were treated with RNase-free DNase I (2 units) at 37˚C for 30 min to remove genomic DNAs, and 10 mg of RNAs were resuspended in water. Random primers, dNTP, 10× RT buffer, and Multiscribe Reverse Transcriptase were then added to the RNA solutions which were then incubated at 25˚C for 10 min followed by 37˚C for 120 min to synthesize the first-strand cDNA. Real-time RT-PCR was performed using a SYBR Green Realtime PCR Master Mix (Takara Bio) and the Applied Biosystems 7900 real-time PCR detection system (ABI, Foster City, CA, USA). Thermal cycling conditions were as follows: first step, 94˚C for 4 min; the ensuing 40 cycles, 94˚C for 1 s, 65˚C for 15 s, and 72˚C for 30 s. The primers used are shown in Table I, and expression of each protein mRNA was normalized by that of glyceraldehyde 3-phosphate dehydrogenase (*GAPDH*) mRNA.

Separation into mitochondrial and cytosolic components. Cells were homogenized with a sonicator in a Buffer A solution (20 mM HEPES, 10 mM KCl, 1.5 mM $MgCl_2$, 1 mM EDTA, 1 mM EGTA, 1 mM dithiothreitol, 0.1 mM phenylmethylsulfonyl fluoride, and 250 mM sucrose, pH 7.5). Lysates were centrifuged at 1,000 × *g* for 10 min, and the supernatant was further centrifuged at 10,000 × *g* for 1 h. The pellet and the supernatant were used as mitochondrial and cytosolic components, respectively.

Western blotting. Samples were loaded onto sodium dodecyl sulfate (SDS)-polyacrylamide gel electrophoresis (PAGE) and transferred to polyvinylidene difluoride membrane. The blotting membrane then reacted to an antibody against cytochrome *c* (Chemicon International, Inc., Temecula, CA, USA), voltage-dependent anion channel 1 (VDAC1) (Santa Cruz Biotechnology, Inc., Dallas, TX, USA) or β-actin (Sigma, St. Louis MO, USA), followed by a horseradish peroxidase (HRP)-conjugated anti-mouse IgG antibody. Immunoreactivity was detected with an ECL kit (Invitrogen, Carlsbad, CA, USA) and visualized using a chemiluminescence detection system (GE Healthcare, Piscataway, NJ, USA). Protein concentrations for each sample were determined with a BCA protein assay kit (Thermo Fisher Scientific, Rockford, IL, USA).

Table I. *Primers used for real-time reverse transcription-polymerase chain reaction.*

Gene	Gene name	Primer	Sequence
BAD	B-cell lymphoma 2-antagonist of cell death	Sense	GCACAGCAACGCAGATGC
		Antisense	AAGTTCCGATCCCACCAGG
BAX	Bcl-2- associated X	Sense	CGGACCCGGCGAGAGGC
		Antisense	TCAGCTTCTTGGTGGACGCATCC
BID	BH3 interacting- domain death agonist	Sense	CTACGATGAGCTGCAGACTG
		Antisense	GATGCTACGGTCCATGCTGTC
PUMA	p53 upregulated modulator of apoptosis	Sense	GACGACCTCAACGCACAGTA
		Antisense	AGGAGTCCCATGATGAGATTGT
HRK	Harakiri, B-cell lymphoma 2 interacting protein	Sense	TGCTCGGCAGGCGGAACTTGTAG
		Antisense	CTTTCTCCAAGGACACAGGG
NOXA	Phorbol-12-myristate-13-acetate- induced protein 1	Sense	GCAGAGCTGGAAGTCGAGTG
		Antisense	GAGCAGAAGAGTTTGGATATCAG
BCL2	B-cell lymphoma 2	Sense	TCCGCATCAGGAAGGCTAGA
		Antisense	AGGACCAAGGCCTCCAAGCT
BCL-XL	B-cell lymphoma- extra	Sense	TGGAATTCATGTCTCAGAGCAACCGGGAGC
		Antisense	CAGAATTCTCATTTCCGACTGAAGAGTGAGC
MCL1	Myeloid cell leukemia 1	Sense	GGACATCAAAAACGAAGACG
		Antisense	GCAGCTTTCTTGGTTTATGG
GAPDH	Glyceraldehyde 3-phosphate dehydrogenase	Sense	GACTTCAACAGCGACACCCACTCC
		Antisense	AGGTCCACCACCCTGTTGCTGTAG

Monitoring of intracellular ATP level. Intracellular ATP levels were assayed using a luminescent ATP detection assay kit containing luciferase and D-luciferin (Wako Pure Chemical Industries, Osaka, Japan). ATP can be relatively quantified by detecting the luminescence signal emitted in luciferase-mediated reaction of D-luciferin with ATP into D-oxyluciferin. Before and after treatment with HUHS1015, cells were incubated in the ATP detection kit for 1 min by shaking, and 10 min later under dark conditions' the emitted light was detected with a microplate reader (ARVO X4; PerkinElmer, Inc., Waltham, MA, USA).

Evaluation of tumor growth in mice inoculated with CW2 cells. Nude BALB/c-nu/nu mice (male, 6 weeks) were obtained from Japan SLC, Inc. (Shizuoka, Japan) (approval number, 12-071). CW2 cells (2×10^6 cells) suspended in 200 ml of culture medium with 50% (v/v) matrigel (BD Biosciences, San Jose, CA, USA) were subcutaneously inoculated into the right flank of 36 mice under general anesthesia with pentobarbital. HUHS1015, and naftopidil were diluted with saline. Saline, HUHS1015, or naftopidil at a volume of 1 μl was intraperitoneally injected twice a week from one week after cell inoculation. The longest (L) and shortest (S) length of inoculated tumors was measured using calipers and tumor volume (V) was calculated according to the following equation: $V=L\times S^2\times0.5$.

Blood (0.3 ml) was collected from each mouse, and blood urea nitrogen, creatinine, aspartate amino transferase, alanine amino transferase were measured by Oriental Yeast Co., Ltd. (Shiga, Japan).

Statistical analysis. Statistical analysis was carried out using unpaired *t*-test, analysis of variance (ANOVA) followed by Fisher's protected least significant difference (PLSD) test, ANOVA followed by a Bonferroni correction, and repeated ANOVA followed by Tukey-Kramer test.

Results

HUHS1015 induces necrosis and apoptosis of Caco-2 and CW2 cells. HUHS1015 reduced cell viability in a concentration (0.3-100 mM)-dependent manner in both Caco-2 and CW2 cells (Figure 1A).

In the TUNEL staining, HUHS1015 increased TUNEL-positive cells both in Caco-2 and CW2 cell lines (Figure 1B and C), indicating HUHS1015 induced apoptosis of Caco-2 and CW2 cells.

In the flow cytometry using PI and AV, PI is a marker of dead cells and AV, by revealing externalized phosphatidyl-serine residues, is a marker of apoptotic cells (9). HUHS1015 increased the populations of PI-positive/AV-negative, PI-negative/AV-positive, and PI-positive/AV-positive cells, which correspond to cells undergoing primary necrosis, early apoptosis, and late apoptosis/secondary necrosis, respectively (10), in both cell lines (Figure 1D and E). This indicates that HUHS1015 induces necrosis and apoptosis of colonic cancer cells.

In the cell-cycle analysis, HUHS1015 significantly increased the proportion of the sub-G_1 phase of cell cycling, corresponding to apoptosis, in both cell lines (Figure 1F and G), supporting the notion of HUHS1015-induced apoptosis of colonic cancer cells.

HUHS1015 induces necrosis of Caco-2 and CW2 cells by reducing intracellular ATP. Mitochondrial damage triggers both

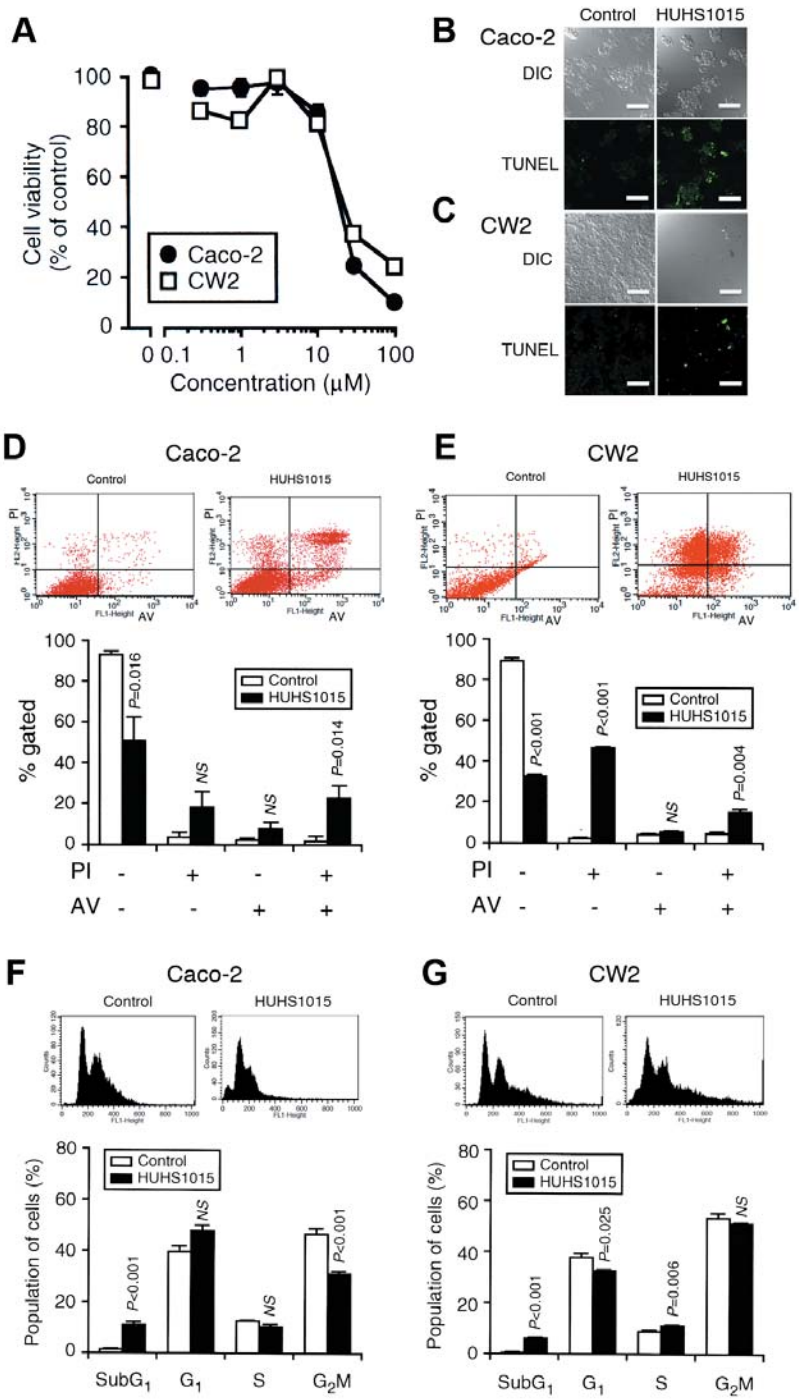

Figure 1. *HUHS1015 induces Caco-2 and CW2 cell death. A: Cells were treated with HUHS1015 at concentrations as indicated for 24 h, and cell viability was assayed with a 3-(4,5-dimethyl-2-thiazolyl)-2,5-diphenyl-2H-tetrazolium bromide (MTT) assay. Data represent the mean (± SEM) percentage of basal levels (MTT intensity of untreated cells) (n=4 independent experiments). B, C: Cells were treated with HUHS1015 (15 mM) for 24 h, followed by terminal deoxynucleotidyl transferase-mediated dUTP nick-end labeling (TUNEL) staining. Note that similar results were obtained with four independent experiments. DIC: Differential interference contrast. Scale bars, 100 mm. D, E: Cells were treated with HUHS1015 (30 mM) for 24 h, followed by flow cytometry using propidium iodide (PI) and annexin V (AV). Typical profiles are shown in the upper panels. In the graphs, each column represents the mean (±SEM) percentage of cells in four fractions against total cells (n=4 independent experiments). p-Values were from unpaired t-test. NS: Not significant. F, G: Cells were treated with HUHS1015 (30 mM) for 24 h, followed by cell-cycle analysis. Typical profiles are shown in the upper panels. In the graphs, each column represents the mean (±SEM) percentage for each phase of cell cycling (n=4 independent experiments). p-Values were from an unpaired t-test. NS: Not significant.*

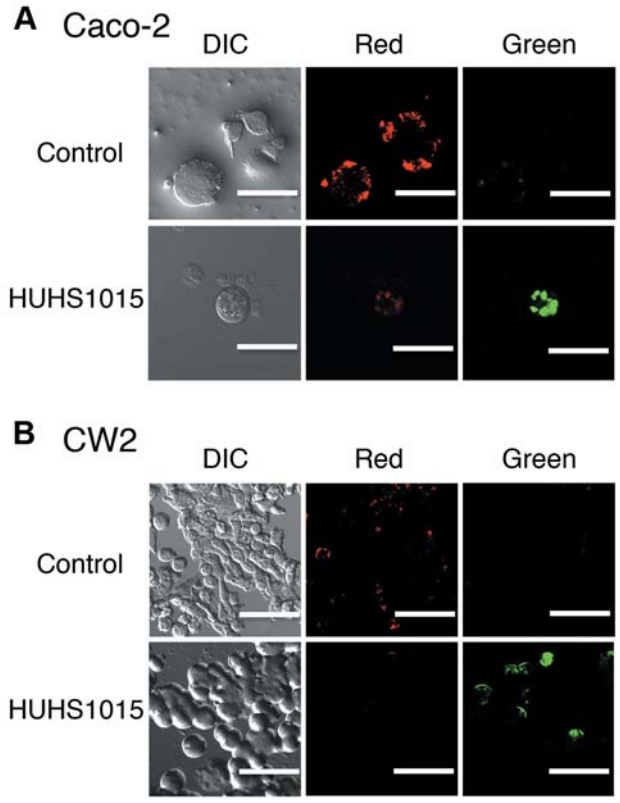

Figure 2. *HUHS1015 disrupts mitochondrial membrane potential. Caco-2 (A) and CW2 cells (B) were untreated (Control) and treated with HUHS1015 (30 mM) for 24 h and the mitochondrial membrane potentials were monitored. DIC: Differential interference contrast. Scale bars, 100 mm. Note that similar results were obtained with four independent experiments.*

necrosis and apoptosis. To determine whether HUHS1015-induced colonic cancer cell death is mediated through mitochondria, we monitored the mitochondrial membrane potential using DePsipher™. For untreated cells, the mitochondria in Caco-2 and CW2 cells exhibited orange-red fluorescent signals at an absorbance of 590 nm and no accumulation of green fluorescent signals at an absorbance of 530 nm (Figure 2A and B). Treatment with HUHS1015 led to accumulation of green fluorescent signals without orange-red fluorescent signals in both cell lines (Figure 2A and B). This indicates that HUHS1015 perturbs the mitochondrial membrane potential.

The mitochondria are the organs that generate ATP. If the mitochondria are damaged, then ATP production should be reduced. Lowering of intracellular ATP levels is known to cause necrosis (11). To address this issue, we monitored intracellular ATP mobilization. HUHS1015 reduced the intracellular ATP concentration in a treatment time (1-6 h)-dependent manner in Caco-2 and CW2 cells, and the effect was significant compared to that of non-treated control cells ($p<0.001$, ANOVA followed by Fisher's PLSD test) (Figure 3A and B). Taken together, these results indicate that HUHS1015 induces necrosis of Caco-2 and CW2 cells by damaging the mitochondria and impairing ATP production.

Death receptors such as tumor necrosis factor-α (TNFα) and its receptor (TNFR) and Fas also damage mitochondria, thereby causing both necrosis and apoptosis. TNFR forms complex I including TNFR-associated death domain protein (TRADD), TNFR-associated factor 2 (TRAF2), receptor-interacting protein 1 (RIP1), and cellular inhibitor of apoptosis 1 (cIAP1) at the cytoplasmic membrane (12). RIP1 is phosphorylated by RIP1 kinase, which forms complex IIb with RIP3, to induce necroptosis (12). Nec-1, an inhibitor of RIP1 kinase, partially inhibited Caco-2 and CW2 cell death induced by HUHS1015 at concentrations higher than 10 mM (Figure 4A and B). This suggests that HUHS1015 may partly induce necroptosis of Caco-2 and CW2 cells.

HUHS1015 induces caspase-dependent apoptosis of Caco-2 and CW2 cells. The B-cell lymphoma 2 (BCL2) family plays a critical role in the regulation of mitochondrial outer-membrane permeabilization. We, therefore, examined the effect of HUHS1015 on the expression of BCL2 family member mRNAs. In the real-time RT-PCR analysis, HUHS1015 increased expression of the BCL2-antagonist of cell death (*BAD*) and BCL2-associated X (*BAX*) as compared with that for non-treated control Caco-2 and CW2 cells, although the effect was not significant (ANOVA followed by Fisher's PLSD test) (Figure 5A and B). In contrast, expression of mRNAs for BH3 interacting-domain death agonist (*BID*), p53 up-regulated modulator of apoptosis (PUMA), harakiri, BCL2 interacting protein (*HRK*), phorbol-12-myristate-13-acetate-induced protein 1 (*NOXA*), BCL2, B-cell lymphoma-extra (*BCL-XL*), and myeloid cell leukemia 1 (*MCL1*) was not affected by HUHS1015 (Figure 5C-I). These results suggest that up-regulation of *BAD* and *BAX* might be implicated in HUHS1015-induced disruption of mitochondrial membrane potential.

When damaged, the mitochondria release a variety of apoptosis-related factors. Out of them we focused on cytochrome *c*. Cytochrome *c* released from the mitochondria binds to apoptotic protease-activating factor 1 (APAF1) followed by dATP, which forms the apoptosome with procaspase-9. Then caspase-9 is activated through its proteolytic processing and in turn, activated caspase-9 activates the effector caspase-3 through its proteolytic processing. HUHS1015 had no effect on total expression of cytochrome *c* proteins in Caco-2 and CW2 cells (Figure 6A and B). We subsequently separated cells into the cytosolic and mitochondrial components. We confirmed *via* western blot analysis using an antibody against VDAC1, a mitochondria-specific protein, that the cytosolic and mitochondrial components were successfully separated. HUHS1015

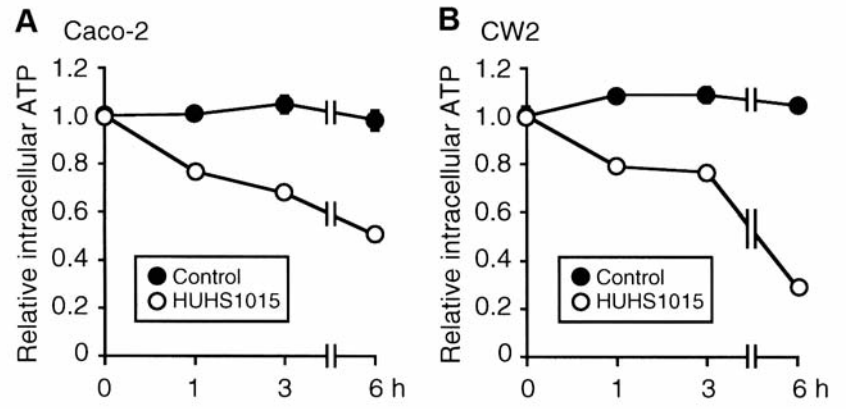

Figure 3. *HUHS1015 reduces the intracellular ATP level. Caco-2 (A) and CW2 cells (B) were untreated (Control) and treated with HUHS1015 (30 mM) for periods of time as indicated, followed by ATP assay. The fluorescence signal at 0 h was regarded as 1. In the graphs, each point represents the mean (±SEM) relative ATP level (n=4 independent experiments).*

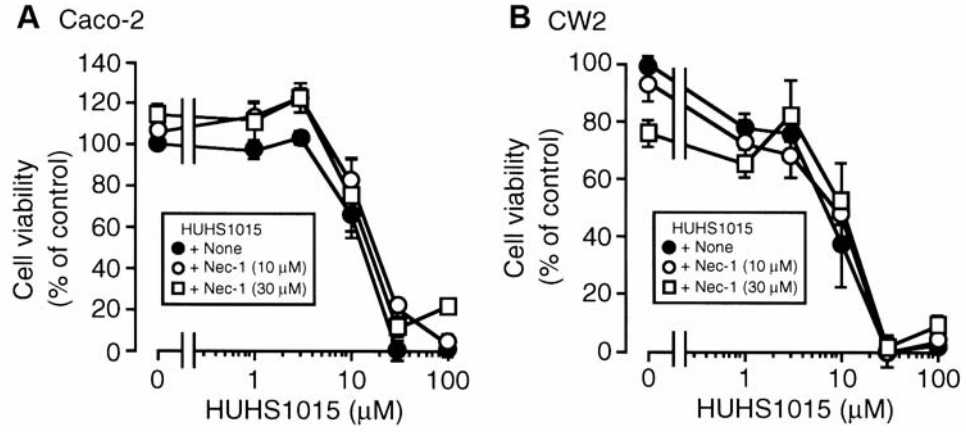

Figure 4. *HUHS1015 in part induces necrosis. Caco-2 (A) and CW2 cells (B) were treated with HUHS1015 at concentrations as indicated in the presence and absence of necrostatin-1 (Nec-1) (10 and 30 mM) for 24 h, followed by 3-(4,5-dimethyl-2-thiazolyl)-2,5-diphenyl-2H-tetrazolium bromide (MTT) assay. Data represent the mean (±SEM) percentage of basal levels (MTT intensities of untreated cells) (n=4 independent experiments).*

increased cytosolic cytochrome *c* in parallel with the reduction of mitochondrial cytochrome c in both cell lines (Figure 6C and D), indicating HUHS1015-induced cytochrome c release from the mitochondria.

To determine whether HUHS1015 activates caspase-9 and the effector caspase-3 following cytochrome *c* release, we assayed caspase activities. HUHS1015 enhanced activities of caspase-3, -4, -8, and -9, the extent reaching nearly 13-, 3-, 2-, and 4-times, respectively, the basal levels at 12-h treatment in Caco-2 cells (Figure 7A). Likewise, HUHS1015 also enhanced activities of caspase-3, -4, -8, and -9, the extent reaching approximately 76-, 12-, 13-, and 16-times, respectively, the basal levels at 12-h treatment in CW2 cells (Figure 7B). These results indicate that HUHS1015 induces apoptosis of Caco-2 and CW2 cells in a caspase-dependent manner. Taken together, these results indicate that HUHS1015 disrupts mitochondrial membrane potentials, allowing cytochrome *c* release from the mitochondria, which causes activation of caspase-9 followed by the effector caspase-3, to induce apoptosis, although it is unknown how HUHS1015 activates caspase-4 and -8.

HUHS1015 suppresses proliferation of CW2 cells. We finally examined the effect of HUHS1015 on tumor growth in mice inoculated with CW2 cells. HUHS1015 or naftopidil was intraperitoneally injected twice a week from one week after inoculation. The tumor volume for control mice injected only with saline increased day by day, reaching over 25-times the initial site on day 36 (Figure 8A and B). HUHS1015 significantly inhibited an increase in the tumor volume compared to that for control mice, while naftopidil had no

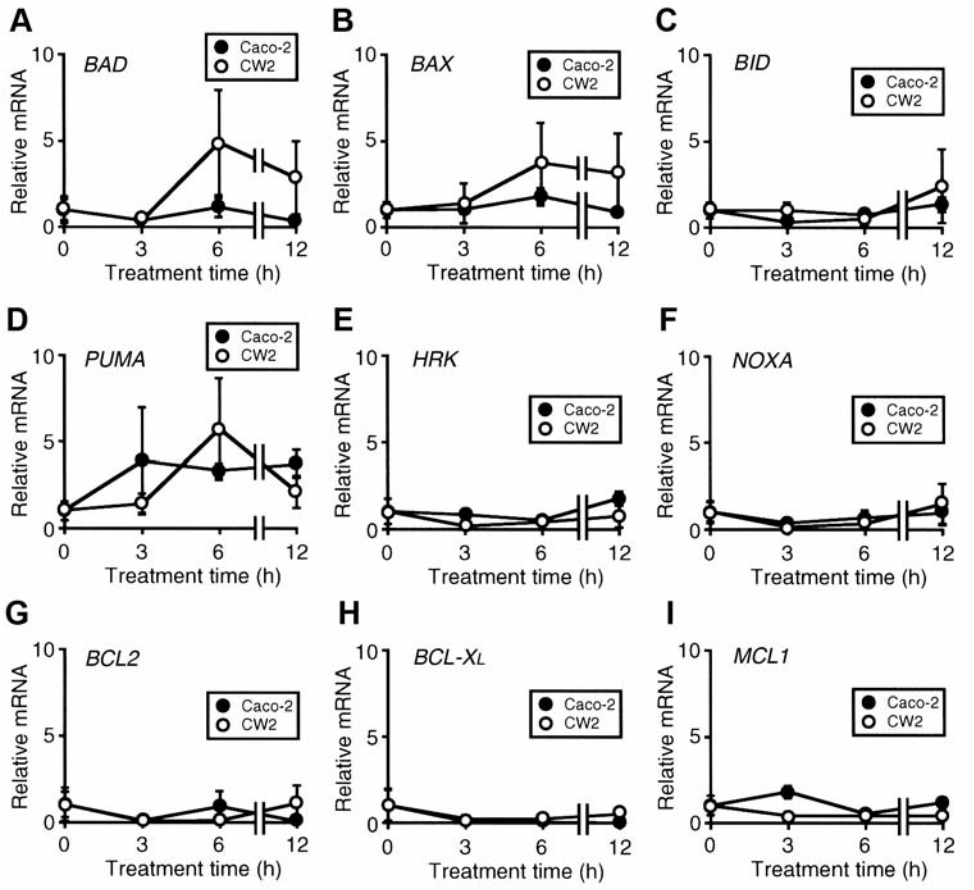

Figure 5. *HUHS1015 up-regulates expression of the BCL2-antagonist of cell death (BAD) and BCL2-associated X (BAX) mRNAs in Caco-2 and CW2 cells. Cells were treated with HUHS1015 (30 mM) for periods of time as indicated, followed by real-time reverse transcription-polymerase chain reaction. The mRNA quantity for each gene was calculated from the standard curve made by amplifying different amount of the glyceraldehyde 3-phosphate dehydrogenase (GAPDH) mRNA, and normalized by regarding the average of independent basal mRNA quantity (0 min) as 1. In the graphs, each column represents the mean (±SEM) ratio relative to the basal mRNA level (n=4 independent experiments).*

significant effect on tumor growth (Figure 8-C). The survival rate throughout experiments was 100% for mice treated with HUHS1015 or naftopidil, although that for control mice was 89% (Figure 8D). No remarkable body weight loss was found throughout experiments in any of the three groups (Figure 8E). In the blood examination on day 36, no renal or liver disturbance was found in mice treated with HUHS1015 mice (Table II). Overall, these results indicate that HUHS1015 effectively suppresses CW2 cell proliferation without side-effects.

Table II. *Blood examination on day 36.*

	Control	HUHUS1015
Blood urea nitrogen (mg/dl)	20±2	21±4
Creatinine (mg/dl)	0.12±0.02	0.10±0.01
Aspartate amino transferase (IU/l)	532±149	533±114
Alanine amino transferase (IU/l)	296±122	329±148

Discussion

In the present study, HUHS1015 reduced cell viability of Caco-2 and CW2 human colonic cancer cell lines in a concentration (0.3-100 mM)-dependent manner. In the flow cytometry using PI and AV, HUHS1015 significantly increased the populations of PI-positive/AV-negative, PI-negative/AV-positive, and PI-positive/AV-positive cells in both cell lines, indicating that HUHS1015 induces primary/secondary necrosis and early/late apoptosis. HUHS1015, on the other hand, markedly increased TUNEL-positive cells and the proportion of the sub-G_1 phase of the cell cycle in both cell lines. These data account for HUHS1015-induced apoptosis. Collectively, HUHS1015 appears to induce both necrosis and apoptosis of colonic cancer cells.

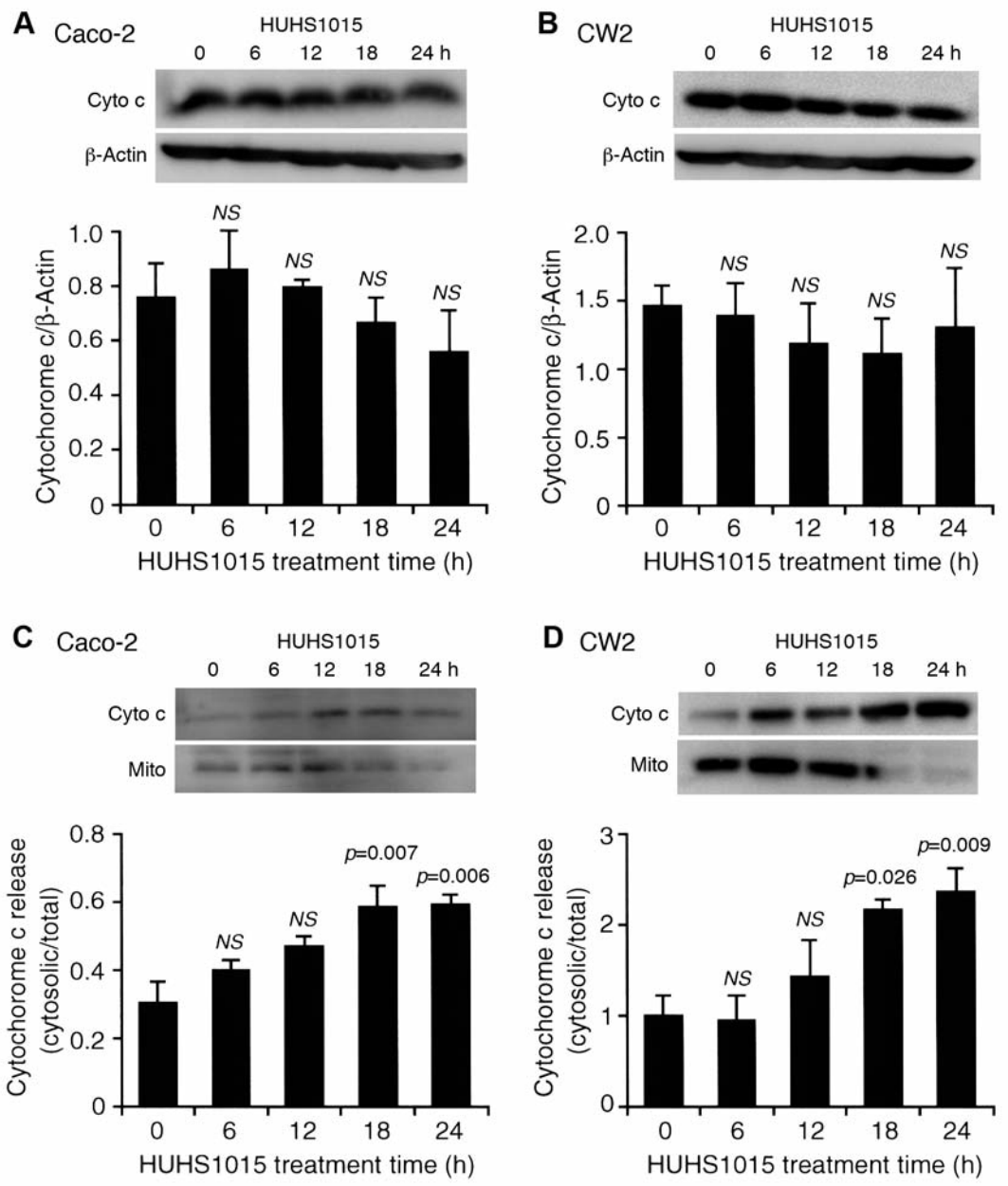

Figure 6. *HUIHS1015 stimulates cytochrome c (Cyto c) release from the mitochondria. Caco-2 (A, C) and CW2 cells (B, D) were treated with HUHS1015 (30 mM) for periods of time as indicated, followed by western blotting of total cell lysates and of the cytosolic (Cyto) and mitochondrial components (Mito). In the graphs, each column represents the mean (±SEM) signal intensity for cytochrome c relative to that for β-actin (n=4 independent experiments) (A, B) or total cytosolic and mitochondrial cytochrome c (n=4 independent experiments) (C, D). p-Values are from ANOVA followed by a Bonferroni correction. N: Not significant.*

HUHS1015 disrupted the mitochondrial membrane potential in Caco-2 and CW2 cells. The mitochondria are central executioners of necrosis and apoptosis. For mitochondria-mediated necrosis, reactive oxygen species (ROS) disrupt the integrity of the mitochondrial inner membrane, to open the mitochondrial permeability transition pore, resulting in reduction of ATP production, responsible for necrosis (13). Oxidative stress, alternatively, causes accumulation of p53 in the mitochondria, to open the pore and induce necrosis (14). It is presently unknown how HUHS1015 damages the mitochondria. The fact that HUHS1015 lowers the intracellular ATP level in a treatment time-dependent manner may support the notion of HUHS1015-induced mitochondria-mediated necrosis of colonic cancer cells.

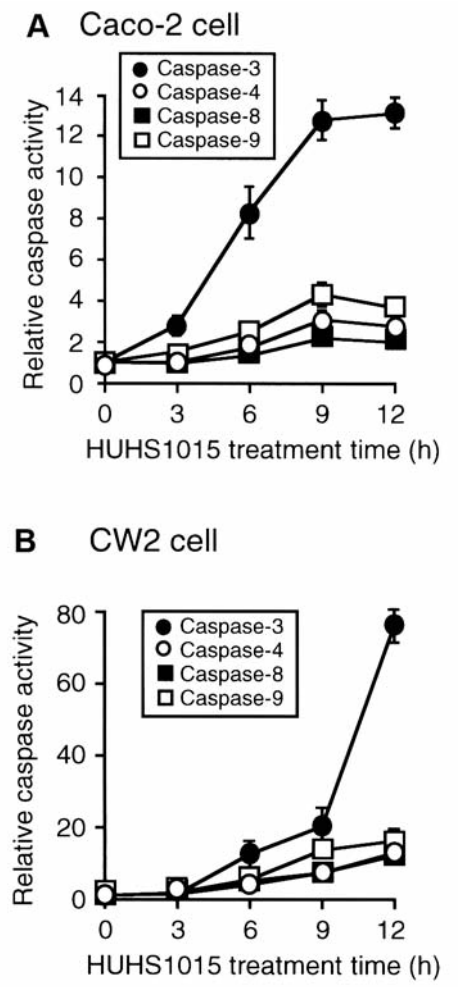

Figure 7. *HUHS1015 activates caspase-3, -4, -8, and -9. Caco-2 (A) and CW2 cells (B) were treated with HUHS1015 (30 mM) for periods of time as indicated, followed by enzymatic caspase assay. In the graphs, each point represents the mean (±SEM) ratio relative to the basal caspase activity (0 h)(n=4 independent experiments).*

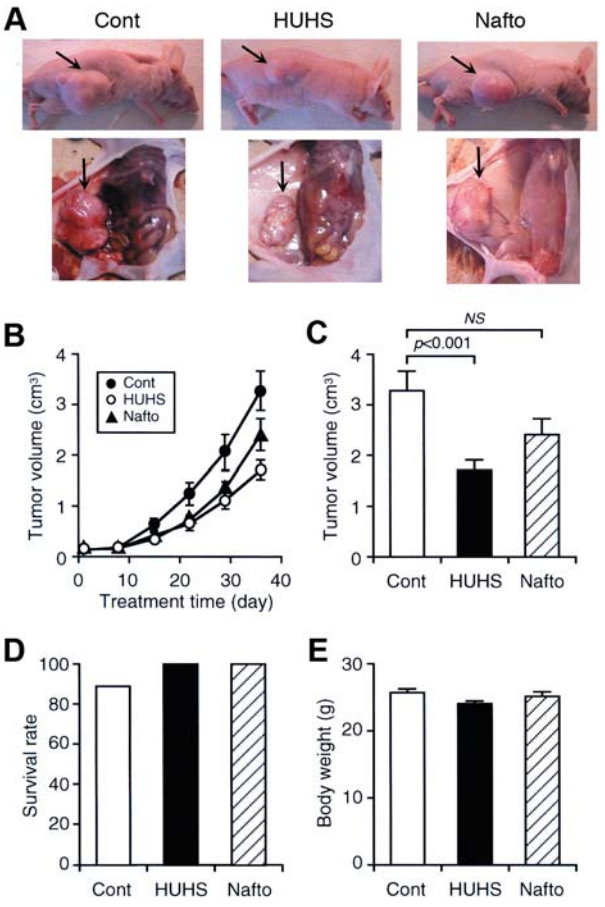

Figure 8. *HUHS1015 suppresses CW2 cell proliferation in mice. CW2 cells were subcutaneously inoculated into the flank of mice, and a week later saline (Cont), HUHS1015 (HUHS: 9.16 mg/kg; ~25 mM), or naftopidil (Nafto: 9.81 mg/kg; ~25 mM) was intraperitoneally injected twice a week. A: External appearance tumor on day 36 and at autopsy (arrows). B: Each data point represents the mean (±SEM) tumor volume at days as indicated (n=8-9 independent mice). C: Each data point represents the mean (±SEM) tumor volume at day 36 (n=8-9 independent mice). p-Values for data compared to control tumor volume were by repeated by ANOVA followed by Tukey-Kramer test. NS: Not significant. D: Each data point represents the survival rate (n=8-9 independent mice). E: Each data point represents the mean (±SEM) body weight on day 36 (n=8-9 independent mice).*

The BCL2 family plays a central role in mitochondria-mediated apoptosis. The BCL2 family is divided into three classes: (i) BCL2 subfamily that includes BCL2, BCL-XL, BCL-w, MCL1, and A1; (ii) BAX subfamily that includes BAX, BAK, and BCL2-related ovarian killer (BOK); and (iii) BH3-only BCL2 family that includes BAD, BCL2-interacting killer (BIK), BID, BCL2-like protein 11 (BIM), BIK-like killer (BLK), HRK, BCL2 19 kDa-interacting protein (BNIP3), PUMA, and NOXA. The BCL2 subfamily serves as anti-apoptotic factors, but otherwise the BAX subfamily and BH3-only BCL2 family serve as pro-apoptotic factors (15, 16). In the real-time RT-PCR analysis, HUHS1015 up-regulated expression of the *BAD* and *BAX* mRNAs. This suggests that BAD and BAX might participate in HUHS1015-induced mitochondria-mediated apoptosis of colonic cancer cells. To address this issue, further investigations are needed.

HUHS1015 activated caspase-3, -4, -8, and -9 in Caco-2 and CW2 cells, and in particular, great activation of caspase-3 was obtained. Out of BCL2 family members BID and BAX make pores in the mitochondria to release apoptosis-related factors, including cytochrome *c*, and induce apoptosis. We, therefore, monitored intracellular localization of cytochrome *c*. As expected, HUHS1015 stimulated cytochrome *c* release from the mitochondria in both cell lines.

Overall, the results of the present study indicate that HUHS1015 disrupted the mitochondrial membrane potential, allowing cytochrome *c* release from the mitochondria and activation of caspase-9 followed by the effector caspase-3, to induce apoptosis of colonic cancer cells. How HUHS1015 activates caspase-4 and -8, however, remains to be explored. Caspase-4 is activated in response to endoplasmic reticulum stress. Caspase-8, on the other hand, is activated mainly through death receptors. TNFR forms complex I of TRADD/TRAF2/RIP1/cIAP1 (11). When activated, TNFR dissociates RIP1/cIAP to recruit and form complex IIa with Fas-associated protein with death domain (FADD) and procaspase-8, leading to activation of caspase-8 (11). RIP1 phosphorylated by RIP1 kinase, alternatively, is dissociated from complex I and forms complex IIb with RIP3, to induce necroptosis (11). In the present study, the RIP1 kinase inhibitor Nec-1 partially inhibited HUHS1015-induced Caco-2 and CW2 cell death. This suggests that HUHS1015 may, in part, induce necroptosis of colonic cancer cells. This also suggests that HUHS1015 might activate caspase-8 by targeting TNFR or its associated proteins.

In the *in vivo* experiments using mice inoculated with CW2 cells, HUHS1015 suppressed tumor growth more effectively than did naftopidil. The survival rate throughout experiments was 100% for mice treated with HUHS1015, without weight loss or renal and liver dysfunction. HUHS1015, thus, could be developed as a promising and safe anticancer drug for treatment of human colonic cancer.

Conclusion

The results of the present study show that HUHS1015 induces both necrosis and apoptosis of Caco-2 and CW2 human colonic cancer cells by lowering the intracellular ATP level and stimulating cytochrome *c* release from the mitochondria, to activate caspase-9 followed by the effector caspase-3, in association with mitochondrial damage. The results also show that HUHS1015 exhibits a beneficial effect against colonic cancer proliferation in the mouse xenograft model.

Conflicts of Interest

None of the Authors have any potential conflict of interest.

References

1 Takei R, Ikegaki I, Shibata K, Tsujimoto G and Asano T: Naftopidil, a novel α_1-adrenoceptor antagonist, displays selective inhibition of canine prostatic pressure and high affinity binding to cloned human α_1-adrenoceptors. Jpn J Pharmacol *79*: 447-454, 1999.

2 Gotoh A, Nagaya H, Kanno T and Nishizaki T: Antitumor action of α1-adrenoceptor blockers on human bladder, prostate, and renal cancer cells. Pharmacology *90*: 242-246, 2012.

3 Masachika E, Kanno T, Nakano T, Gotoh A and Nishizaki T: Naftopidil induces apoptosis in malignant mesothelioma cell lines independently of α_1-adrenoceptor blocking. Anticancer Res *33*: 887-894, 2014.

4 Kanno T, Tanaka A, Shimizu T, Nakano T and Nishizaki T.1-[2-(2-Methoxyphenylamino)ethylamino]-3-(naphthalene-1-yloxy)propan-2-ol as a potential anticancer drug. Pharmacology *91*: 339-345, 2013.

5 Kaku Y, Nagaya H, Tsuchiya A, Kanno T, Gotoh A, Tanaka A, Shimizu T, Nakao S, Tabata C, Nakano T and Nishizaki T: Newly synthesized anticancer drug HUHS1015 is effective on malignant pleural mesothelioma. Cancer Sci *105*: 883-889, 2014.

6 Kaku Y, Tsuchiya A, Kanno T, Nakao S, Shimizu T, Tanaka A and Nishizaki T: The newly synthesized anticancer drug HUHS1015 is useful for treatment of human gastric cancer. Cancer Chemother Pharmacol *75*: 527-535, 2015.

7 Kaku Y, Tsuchiya A, Kanno T and Nishizaki T: HUHS1015 induces necroptosis and caspase-independent apoptosis of MKN28 human gastric cancer cells in association with AMID accumulation in the nucleus. Anticancer Agents Med Chem *15*: 242-247, 2015.

8 Saitoh M, Nagai K, Nakagawa K, Yamamura T, Yamamoto S and Nishizaki T: Adenosine induces apoptosis in the human gastric cancer cells via an intrinsic pathway relevant to activation of AMP-activated protein kinase. Biochem Pharmacol *67*: 2005-2011, 2004.

9 Vanags DM, Pörn-Ares MI, Coppola S, Burgess DH and Orrenius S: Protease involvement in fodrin cleavage and phosphatidylserine exposure in apoptosis. J Biol Chem *271*: 31075-1085, 1996.

10 Pietra G, Mortarini R, Parmiani G and Anichini A: Phases of apoptosis of melanoma cells, but not of normal melanocytes, differently affect maturation of myeloid dendritic cells. Cancer Res *61*: 8218-8226, 2001.

11 Zong WX and Thompson CB: Necrotic death as a cell fate. Genes Dev *20*: 1-15, 2006.

12 Christofferson DE and Yuan J: Necroptosis as an alternative form of programmed cell death. Curr Opin Cell Biol *22*: 263-268, 2010.

13 Griffiths EJ and Halestrap AP: Mitochondrial non-specific pores remain closed during cardiac ischaemia, but open upon reperfusion. Biochem J *307*: 93-98, 1995.

14 Vaseva AV, Marchenko ND, Ji K, Tsirka SE, Holzmann S and Moll UM: p53 opens the mitochondrial permeability transition pore to trigger necrosis. Cell *149*: 1536-1548, 2010.

15 Zhang LN, Li JY and Xu W: A review of the role of Puma, Noxa and Bim in the tumorigenesis, therapy and drug resistance of ± chronic lymphocytic leukemia. Cancer Gene Ther *20*: 1-7, 2013.

16 Tomek M, Akiyama T and Dass CR: Role of Bcl-2 in tumour cell survival and implications for pharmacotherapy. J Pharm Pharmacol *64*: 1695-1702, 2012.

Received October 9, 2015
Revised November 9, 2015
Accepted November 24, 2015